



Characterisation of the Sensitisation Behaviour of Thermo-mechanically Processed Type 304 Stainless Steel Using DL-EPR Testing and Image Analysis Methods

[Link to publication record in Manchester Research Explorer](#)

Citation for published version (APA):

Rahimi, S., Engelberg, D. L., & Marrow, T. J. (2010). Characterisation of the Sensitisation Behaviour of Thermo-mechanically Processed Type 304 Stainless Steel Using DL-EPR Testing and Image Analysis Methods. In *host publication*

Published in:
host publication

Citing this paper

Please note that where the full-text provided on Manchester Research Explorer is the Author Accepted Manuscript or Proof version this may differ from the final Published version. If citing, it is advised that you check and use the publisher's definitive version.

General rights

Copyright and moral rights for the publications made accessible in the Research Explorer are retained by the authors and/or other copyright owners and it is a condition of accessing publications that users recognise and abide by the legal requirements associated with these rights.

Takedown policy

If you believe that this document breaches copyright please refer to the University of Manchester's Takedown Procedures [<http://man.ac.uk/04Y6Bo>] or contact uml.scholarlycommunications@manchester.ac.uk providing relevant details, so we can investigate your claim.



CHARACTERISATION OF THE SENSITISATION BEHAVIOUR OF THERMO-MECHANICALLY PROCESSED TYPE 304 STAINLESS STEEL USING DL-EPR TESTING AND IMAGE ANALYSIS METHODS

S. Rahimi¹, *D.L. Engelberg¹, T.J. Marrow¹

¹ Materials Performance Centre, School of Materials, University of Manchester,
Oxford Road, Manchester, M13 9PL, UK

Abstract

Standard test methods such as the Electrochemical Potentiokinetic Reactivation Test (EPR – ASTM G108) and the Double-Loop EPR test (DL-EPR – ISO12732) are commonly used to characterise sensitisation behaviour in austenitic stainless steels. These tests provide a quantitative assessment of microstructure susceptibility. Factors such as different grain size may be accounted for, but additional information on the network of sensitised boundaries is neglected. This paper reports a new approach to characterise the development of sensitisation, applied to a Type 304 austenitic stainless steel subjected to thermo-mechanical processing. DL-EPR testing is augmented by large area Image Analysis (IA) assessments of optical images to measure the dimensions and connectivity of the attacked grain boundary network. Comparison is made with the standard assessment methods, and a new method is proposed, based on normalisation by a cluster parameter to describe the network of susceptible grain boundaries. This parameter can be estimated by electron backscatter diffraction (EBSD) methods in the non-sensitised condition. The proposed method allows a simple quantitative assessment of the degree of sensitisation of different microstructures and heats of austenitic stainless steels.

Keywords

DL-EPR, Image Analysis (IA), Intergranular Corrosion (IGC), Sensitisation, Austenitic Stainless Steels

1 Introduction

Sensitisation of stainless steels is related to chromium depletion near grain boundaries. This results in intergranular corrosion (IGC) or intergranular stress corrosion cracking (IGSCC) [1], and may occur in service after heat treatment (e.g. post weld and stress relief) or fast neutron irradiation [2, 3]. The need for a rapid, non-destructive and quantitative approach to determine the degree of sensitisation (DOS) in stainless steels and nickel based alloys led to the development of the Electro-chemical Potentio-kinetic Reactivation (EPR) test [4]. EPR testing can be carried out using a single loop test (SL-EPR) [5], the double loop test (DL-EPR) [6, 7], or in the form of a simplified EPR procedure using a combination of features from the SL-EPR and DL-EPR test methods [8]. In assessing the DOS by the DL-EPR test, the polarisation curve that applies to the matrix (i.e. the activation loop) is distinguished from that pertaining to the susceptible chromium depleted grain boundaries (i.e. the reactivation loop) [4].

This paper addresses a new way to assess DL-EPR test data for evaluation of the DOS in thermo-mechanically processed austenitic stainless steel. Results from standard DL-EPR assessment methods [9, 10] are compared to methods using the measured length and area of the attacked grain boundary network obtained using image analysis (IA) of micrographs recorded from a large area, relative to the microstructure length-scale. The influence of the “cluster compactness” [11] of the attacked grain boundary network on assessment of the DOS is also addressed, with the objective of quantifying the level of sensitisation of susceptible grain boundaries directly from the DL-EPR test.

2 Experimental Procedures

A mill annealed Type 304 austenitic stainless steel (UNS30400) plate with a chemical composition of (wt.%) 18.15Cr–8.60Ni–0.45Si–1.38Mn–0.055C–0.032P–0.038N–0.005S was used in this investigation. Rectangular specimens with dimensions of 210×15×13 mm ($L \times W \times T$) were cut from the as-received plate and solution annealed at 1050°C for 2 hours in argon atmosphere. Thermo-mechanical treatments were carried out on the solution annealed material. Samples were strained along the (L) direction to 5%, 10%, 20% and 30% strain, using a crosshead displacement rate of 2 mm/min, before heat treatment at 900°C and 950°C for up to 26 hours. The thermo-mechanical treatments are reported in this paper by their percentage of tensile deformation, annealing temperature and annealing time. For instance 30%/950/26 represents 30% deformation, followed by an annealing treatment at 950°C for 26 hours. Samples from the as-received (As-Rec) and solution annealed (SA) microstructures were also kept for comparison. A selection of microstructures were sensitised at 650°C for up to 20 hours.

The sensitised samples were DL-EPR tested in a de-aerated solution of 0.5 M H₂SO₄ + 0.01 M KSCN at ambient temperature [7, 10]. A platinum counter electrode and a saturated calomel reference electrode (SCE) were used for the potentiodynamic EPR tests, applying a sweep rate of 1.667 mV s⁻¹. Data from these tests were evaluated with standard assessment methods comprising, (i) ratios of maximum currents of re-activation (I_r) polarisation sweep and the anodic activation (I_a) sweep [7, 8, 10], (ii) ratios normalized by the estimated dimension of the susceptible grain boundary network length, $(I_r/I_a)_{GBL}$ [10], and (iii) ratios normalized by the estimated dimension of the area of the susceptible GB network, $(I_r/I_a)_{GBA}$ [10]. The length of the potentially susceptible grain boundary network is estimated in the two latter methods by converting the measured grain size (excluding twin grain boundaries) into a grain boundary length. The susceptible grain boundary area is then determined by assuming a constant and uniform width of boundary attack (10-4 cm) [10]. Assessment of the susceptible boundary length and area results in the same ranking of DOS for microstructures, as the parameters are directly related to each other. The three assessment methods to calculate the DOS are given in Equation 1, Equation 2 and Equation 3, respectively [10]. The standardised method given in Equation 2 and Equation 3 is known as Cihal's method [10].

$$\text{DOS} = I_r/I_a \quad \text{Equation 1}$$

$$\left(\frac{I_r}{I_a}\right)_{GBL} = \frac{I_r/I_a}{L_{GBL}/A_s} = \frac{I_r/I_a}{10L_A A_s/A_s} = \frac{I_r}{10L_A I_a} = \frac{I_r}{I_a 10\sqrt{2}^{G+3}} \times 10^4 \text{ (}\mu\text{m)} \quad \text{Equation 2}$$

$$\left(\frac{I_r}{I_a}\right)_{GBA} = \frac{I_r/I_a}{S_{GBA}/A_s} = \frac{I_r/I_a}{S_A A_s/A_s} = \frac{I_r}{I_a S_A} = \frac{I_r}{I_a 10^{-3}\sqrt{2}^{G+3}} \quad \text{Equation 3}$$

I_r : Maximum current density of the reactivation curve ($\mu\text{A}\cdot\text{cm}^{-2}$)

I_a : Maximum current density of the anodic polarisation curve ($\mu\text{A}\cdot\text{cm}^{-2}$)

A_s : Total exposed surface area or specimen surface area (cm^2)

S_A : Grain boundary area per unit of specimen area ($S_A = 4 \times 10^{-3}\sqrt{2}^{G+1}$).

G : Grain size number that is available in BS ISO 643 [12]. Note that the grain size number has been calculated by excluding the twin grain boundaries.

S_{GBA} : Total grain boundary area, $S_{GBA} = S_A \times A_S$.

L_{GBL} : Total length of grain boundaries, $L_{GBL} = 10 \times L_A \times A_S$ (cm).

L_A : Length of grain boundary per unit of specimen area, $L_A = \sqrt{2G^2 + S}$ (mm⁻¹).

Optical images of the attacked surfaces were obtained after DL-EPR testing. Individual images each with a dimension of 1100 μm × 880 μm were stitched together using Adobe Photoshop CS, to create a single high-resolution image with a total surface area of 18 mm². Image analysis (IA) (MatLab 7.0.1) was used to segment the attacked regions. The total area of the attacked surface, which was predominantly intergranular, was determined, and the average width of attacked grain boundary for each microstructure was obtained. The attacked grain boundary length was then estimated by dividing the total attacked area by the mean attacked boundary width. These measurements of the actual grain boundary attack were then used to normalize the DOS ratio from DL-EPR testing, and these results were compared to results obtained using the estimated length and area of attack (Equation 2 and Equation 3).

The dimension of the largest connected cluster, M , in each microstructure was obtained from the image analysis and was used to calculate the cluster compactness (C) of the network of attacked grain boundaries. This geometrical parameter has been proposed to describe the break-up of the network of corrosion susceptible grain boundaries [11]. The cluster compactness is given in Equation 4.

$$C = \frac{L_M \cdot D}{A}$$

Equation 4

Where L_M is the length of maximum cluster of attacked chromium depleted boundaries, D is the grain size (disregarding twins) and A is the area of the smallest square that bounds the maximum cluster.

3 Results and Discussion

The development of the DOS as a function of sensitisation time, (Equation 1), is summarized in Figure 1. The DOS increases with sensitisation time, and approaches saturation with longer exposures (>8 hrs). Optical micrographs confirmed that the microstructures are fully sensitised condition after 20 hours at 650°C. The grain sizes of the As-Rec, SA, 20%/950/26 and 30%/950/26 microstructures obtained using EBSD maps (each comprising more than 3000 grains), are 21 ± 2 μm, 59 ± 6 μm, 34 ± 1 μm and 23 ± 2 μm [11]. The grain boundary character distributions (GBCD) were assessed previously [11], with length fractions of low Σ CSL boundaries (Σ≤29) from $54 \pm 1\%$ for the As-Rec microstructure to $65 \pm 2\%$ for the SA and 20/950/26 microstructures.

The DOS was normalized by the estimated grain boundary length and boundary area using Equation 2 and Equation 3. For direct comparison, the DOS was also normalized using the attacked grain boundary length and boundary area, measured by the image analysis assessment. The data, as a function of sensitisation time, are presented in Figure 2. Generally the attacked grain boundary length is smaller than the grain boundary length estimated by Cihal's method. This gives a higher normalised DOS using the measured length of attack. In contrast, the grain boundary area of attack estimated by Cihal's method is smaller than the measured attacked boundary area. The measured grain boundary length and grain boundary area increased with sensitisation time, consistent with previous observations of the measured area of attacked grain boundaries [13].

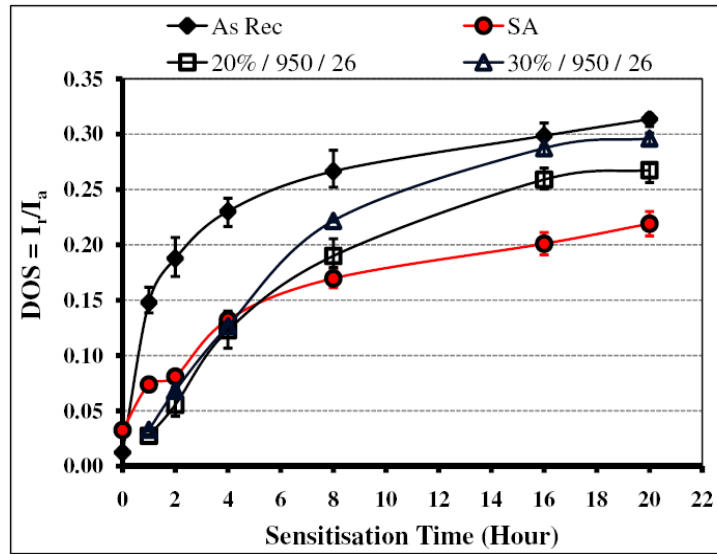


Figure 1: Degree of sensitisation (DOS) as a function of sensitisation time at 650°C. The error bars describe the maximum and minimum of three DL-EPR tests.

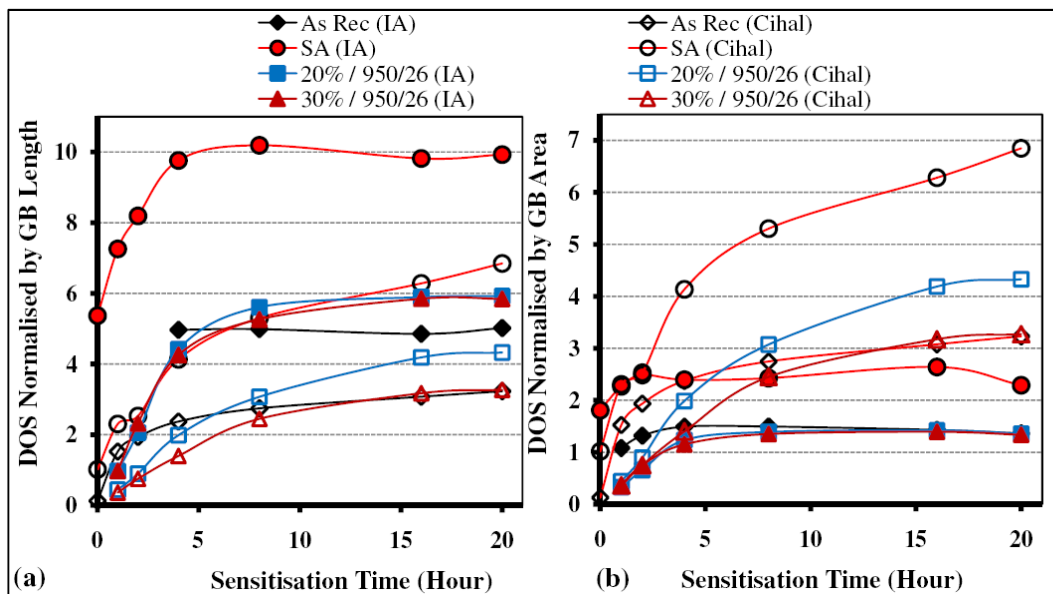


Figure 2: Normalised current ratios (DOS) as functions of sensitisation time at 650°C by (a) length of attacked boundaries measured using IA, and estimated grain boundary length (Cihal's method), and (b) area of attacked boundaries measured using IA, and estimated area of attacked boundaries (Cihal's method).

Normalization by Cihal's method, which estimates the attacked grain boundary length and area from the grain size requires several assumptions. Firstly, it is assumed that the reactivation current, I_r , is associated with grain boundary sensitisation only. Hence the contributions of corrosion at inclusions, δ -ferrite/austenite interfaces, and attacked slip bands are neglected. Secondly, the rate of sensitisation of all grain boundaries is

considered equal. Thirdly, the width of attack of all grain boundaries is assumed constant ($10^{-4}cm$) [10]. However, the sensitisation behaviour depends on the crystallographic structure of grain boundaries [3, 14-16], so these assumptions may become inappropriate when comparing microstructures with different grain boundary character distributions.

To investigate the wider applicability of the image analysis method, a range of thermo-mechanical process treatments, conducted using the same Type 304 material and the same sensitisation treatments (20 hrs at 650°C), were tested. The average grain sizes ranged between 14 and 77 μm . Full details of the thermo-mechanical treatments and microstructure data are given elsewhere [11]. The DL-EPR ratios were normalized by the estimated length and area of attacked grain boundaries (Cihal's method), and also using the measured length and area from image analysis. These are compared in Figure 3, in which the four microstructures from Figure 1 and Figure 2 are highlighted.

The normalizations obtained by measured or estimated area (Figure 3b) do not show a clear trend. This is partly due to variation in the attacked width of the grain boundaries, neglected by Cihal's method. The DOS normalized by the measured attacked grain boundary length is higher than that obtained by Cihal's method (Figure 3a), as noted previously. The degree of this enhancement is variable, however, but may be understood from differences in the grain boundary network, described by the cluster compactness.

The cluster compactness [11] measures the break-up of the network of corrosion susceptible grain boundaries. As compactness decreases, a smaller fraction of boundaries are corrosion susceptible. Figure 4a compares the DOS normalized by the measured attacked grain boundary length, with that normalized by the Cihal estimate of grain boundary length, here modified by the cluster compactness. In this case, the cluster compactness is obtained by analysis of optical images, and is denoted C_{OIA} . The agreement is good, as both C_{OIA} and the attacked grain boundary length are essentially derived from the same observations. The normalised DOS also gives the corrosion current per unit length of attacked grain boundary, and this may be used to assess the degree of sensitisation of the attacked grain boundaries in the microstructure.

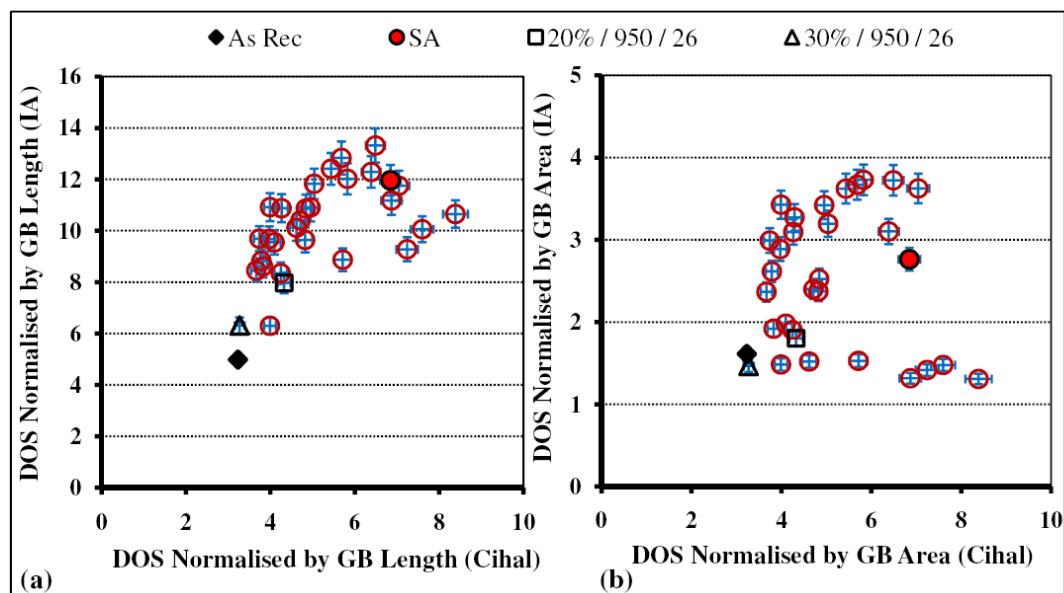


Figure 3: Comparison of the DOS normalised by estimated (Cihal's method) and measured grain boundary attack (IA) for (a) the length of attacked grain boundary and (b) area of attacked grain boundaries.

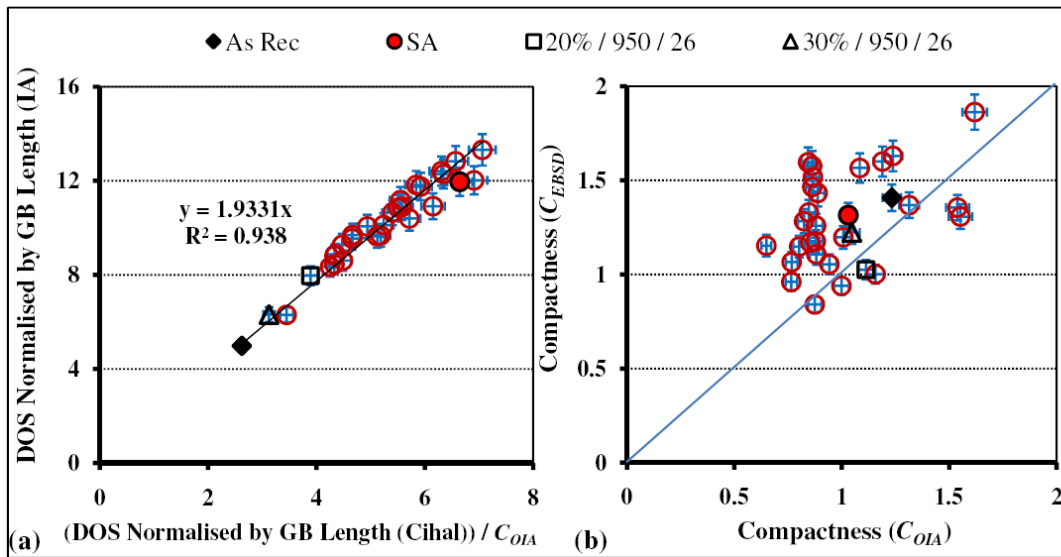


Figure 4: (a) Comparison between the DOS obtained by DL-EPR testing normalised by the attacked grain boundary length (measured using IA) to the DOS normalised by the estimated grain boundary length (Cihal's method) modified by cluster compactness (C_{OIA}). (b) Comparison of the compactness of the attacked boundary network (C_{OIA}) to the compactness of the network of potentially susceptible boundaries ($\Sigma > 29$) from EBSD analysis (C_{EBSD}).

The image analysis (IA) approach is thus proposed to give more accurate measure of the microstructure's degree of sensitisation, since it is a direct measurement of the corroded grain boundaries. It is sensitive to some possible errors, which arise from segmentation of the images to measure the corroded area. Corrosion pits and attacked slip bands that contribute to the reactivation current (I_r) may be included in the attacked grain boundary measurement. This can significantly influence measurements in cold worked materials. Features developed during the anodic polarisation loop may also be included in the measurement of corrosion during reactivation. These contributions increase scatter.

It is interesting to compare the cluster compactness, C_{OIA} , for fully sensitised microstructures with the parameter, C_{EBSD} , derived similarly from image analysis of the high Σ ($\Sigma > 29$) boundary network obtained from EBSD maps (Figure 4b). C_{EBSD} , which is a function of the thermo-mechanical processing of the microstructure, depends on the degree of twinning. Twin growth breaks up of the network of sensitisation-susceptible grain boundaries [17]. The two measures of compactness are therefore correlated. In principle, the value of C_{OIA} in a fully sensitised microstructure may be estimated from measurement of C_{EBSD} , without image analysis of a tested sample. A modification of the Cihal method assessment, using C_{EBSD} , may thus provide a more accurate method for characterising sensitisation, by providing a better estimate of the attacked grain boundary length.

4 Conclusion

- A new approach for measurement of the degree of sensitisation, with the DL-EPR test has been introduced, using normalisation by image analysis (IA) of the clusters of attacked grain boundaries. This new approach is compared with the standard normalisation approach (Cihal's method), which can overestimate the length of attacked grain boundaries.

- This new approach can measure the degree of sensitisation of the attacked grain boundaries, and this may be used to compare sensitisation of differently thermo-mechanically processed microstructures and alloys.

REFERENCES

- [1] - P. M. Scott (2000). Stress corrosion cracking in pressurized water reactors - interpretation, modelling, and remedies. *Corrosion*, Vol.56, p.771-782.
- [2] - S. M. Bruemmer, G. S. Was (1994). Microstructural and microchemical mechanisms controlling intergranular stress corrosion cracking in light-water-reactor systems. *J. Nucl.Mater*, Vol.216, p.348-363.
- [3] - Y. Zhou, K. T. Aust, U. Erb, G. Palumbo (2001). Effects of grainboundary structure on carbide precipitation in 304L stainless steel. *Scr. Mater.*, Vol.45 (1), p.49-54.
- [4] - V. Cihal, R. Stefec (2001). On the development of the electrochemical potentiokinetic method. *Electrochimica Acta*, Vol.46, p.3867-3877.
- [5] - W. L. Clarke, V. M. Romero, J. C. Danko (1977), Detection of sensitisation in stainless steels using electrochemical techniques, Houston, Texas: NACE/77, National Association of Corrosion Engineers.
- [6] - M. Akashi, T. Kawamoto, F. Umemura (1980). Evaluation of IGSCC susceptibility of austenitic stainless steels using electrochemical reactivation method. *Corrosion Engineering*, Vol.29, p.163.
- [7] - A. P. Majidi, M. A. Streicher (1984). The double loop reactivation test for detecting sensitisation in type 304 and 304L stainless steels. *Corrosion (Houston)*, Vol.40, p.584.
- [8] - A. P. Majidi, M. A. Streicher (1986). Four Nondestructive Electrochemical Tests for Detecting Sensitisation in Type 304 and 304L Stainless Steels. *Nuclear Technology*, Vol.75, p.356 - 369.
- [9] - ASTM G108 Electrochemical Reactivation (EPR) for Detecting Sensitisation of AISI Type 304 and 304L Stainless Steels, 1999.
- [10] - British Standard (BS ISO 12732), Corrosion of metals and alloys - Electrochemical potentiokinetic reactivation measurement using the double loop method (based on Cihal's method), 2006.
- [11] - S.Rahimi, D.L. Engelberg, T.J. Marrow (accepted), Characterisation of Grain Boundary Cluster Compactness in an Austenitic Stainless Steel, *J. Mat. Sci. & Tech.*
- [12] - British Standard (BS EN ISO 643), Steels - Micrographic determination of the apparent grain size, 2003.
- [13] - D. B. Wells, J. Stewart, A. W. Herbert, P. M. Scott, D. E. Williams (1989). The use of percolation theory to predict the probability of failure of sensitised austenitic stainless steels by intergranular stress corrosion cracking. *Corrosion*, Vol.45 (8), p.649.
- [14] - V. Y. Gertsman, S. M. Bruemmer (2001). Study of grain boundary character along intergranular stress corrosion crack paths in austenitic alloys. *Acta Mater*, Vol.49, p.1589-1598.
- [15] - S. Rahimi, D. L. Engelberg, J. A. Duff and T. J. Marrow (2009). In situ observation of intergranular crack nucleation in a grain boundary controlled austenitic stainless steel. *J. Microsc*, Vol.233 (3), p.423-431.
- [16] - H. Kokawa, M. Shimada, Y. S. Sato (2000). Grain-boundary structure and precipitation in sensitized austenitic stainless steels. *J. Miner. Metals Mater. Soc.*, Vol.52 (7), p.34-37.
- [17] - A. King, G. Johnson, D. L. Engelberg, T. J. Marrow, W. Ludwig (2008). Observations of Intergranular Stress Corrosion Cracking in a Grain-Mapped Polycrystal. *Science*, Vol.321 (5887), p.382 - 385.